



 Cite this: *RSC Adv.*, 2021, 11, 35703

Effects of mixing temperature on the extrusion rheological behaviors of rubber-based compounds

 Zhongjin Du,^{ab} Yu Du,^{ab} Yankun Gong,^a Guizhi Liu,^a Zhuo Li,^b *a Guangshui Yu^a and Shugao Zhao^a

In this study, rim strip (R) and sidewall (S) compounds were prepared at varying initial mixing temperatures. The effects of the mixing temperature on the extrusion rheological behaviors of the compounds were investigated, and the relationships between the compound structure and the extrusion rheological behaviors were studied. The results showed that the tensile stress relaxation rates of both R and S were more sensitive to the mixing temperature than the shear stress relaxation rate, and the former was affected by both the dispersion of carbon black (CB) and the actual molecular weight of the rubbers. Strain sweep results showed that R, which had a higher CB content, had a more obvious Payne effect than S. When the initial mixing temperature increased from 80 °C to 90 °C, both storage modulus (G') at a low shear strain and the $\Delta G'$ of R obviously decreased, indicating CB dispersion improvement. The S extrudates showed higher die swell ratios (B) than the R extrudates, and the former was more sensitive to mixing temperature. The main factors influencing the B of the R and S were the CB dispersity and the molecular weight, respectively. In addition, at high extrusion rates, a sharkskin phenomenon could be observed for the R extrudate surfaces, whereas the S extrudates were more likely to be integrally distorted.

 Received 5th August 2021
 Accepted 28th October 2021

DOI: 10.1039/d1ra05929g

rsc.li/rsc-advances

1 Introduction

Extrusion is a common approach in polymer processing.^{1–3} In particular, a variety of rubber products, such as tire treads/sidewalls,^{4–6} seal strips,^{7,8} wires⁹ and hoses^{10,11} are obtained by the extrusion process. Rubber is a type of viscoelastic material, which means it exhibits both viscous and elastic characteristics when undergoing deformation. These two characteristics affect industrial extruding production in different ways. Specifically, viscous flow is associated with the production rate, whereas the elastic property of rubber influences the appearance and dimensional stability of the extrudates,¹² which further determines the quality and cost of the final products.¹³ Some familiar phenomena, for example, die swell and distortion of the extrudate, are considered to be caused by elastic memory.^{12,14,15} In recent decades, the rheological behaviors of this viscoelastic rubber material have attracted increasing attention from academia.^{16–18} It is worth noting that the rubber compounds were mostly prepared from rubber composites with a complex formula, and thus their rheological behaviors were influenced by multiple factors. In addition to the rubber structure,^{19–22} the characteristics, content and introduction method of the ingredients (curing system, fillers, plasticizers, *etc.*),^{23–28} as integral

parts of rubber composites, play a significant role in determining the rheological behaviors of the composites. For example, Patcharaphun *et al.*²³ concluded that the viscosity of rubber compounds utilizing conventional and efficient vulcanizing systems was lower than that of compounds with non-sulfur systems at any given shearing rate. Furthermore, the mixing process parameters should be carefully controlled since the improper process may lead to issues such as filler aggregation or scorching and thus worsen the rheological properties and aggravate the appearance defects of the extrudates. Studies conducted by Li²⁹ demonstrated that mixing time could affect the die swell ratio (B) of the compounds by influencing the dispersity of carbon black (CB).

In addition, it is widely accepted that the extruding process is another decisive factor for extrudates. For industrial manufacture, a screw extruder is applied for extrusion; the screw length-to-diameter ratio (L/D) and configuration,^{30,31} the barrel temperature,³² the screw rotating speed,³³ the feed rate³⁴ and the die shape³⁵ are set according to the material characteristics and the requirements for both the quality and efficiency of the output. In laboratory studies, a capillary rheometer is normally used for rheological behavior investigations.^{36–39}

Coextrusion is a process that simultaneously extrudes two or more materials together through one common die system to create a multilayered extrudate.^{14,40} It is widely applied in actual tire manufacturing. Defects of the coextrudates are more prone to occur if the rheological properties of the component parts, such as the rim strip and sidewall compounds, are significantly

^aKey Laboratory of Rubber-Plastics, Ministry of Education, Shandong Provincial Key Laboratory of Rubber-Plastics, Qingdao University of Science & Technology, Qingdao 266042, China. E-mail: lizhuoqust@126.com

^bInstitute of Polymer Materials and Plastics Engineering, TU Clausthal, Agricolastr. 6, Clausthal-Zellerfeld 38678, Germany



different. It is essential to understand the rheological performance of each part in the coextrusion to optimize the mixing and extrusion process. In this study, two rubber composites with different formulas (with the characteristics of rim strip and sidewall components) were prepared at various initial mixing temperatures in the internal mixer. Their rheological performances were systematically investigated; the effects and their mechanisms of the mixing temperature were discussed.

2 Experimental

2.1 Materials

Natural rubber (NR, TSR 9710, number-average molecular weight (M_n) = 2.4×10^5 , weight-average molecular weight (M_w) = 6.5×10^5) was supplied by Hainan Sinochem Rubber Co., Ltd., Hainan, China. Butadiene rubber (BR, BR9000, $M_n = 1.0 \times 10^5$, $M_w = 3.5 \times 10^5$) was provided by Chuanhua Synthetic Material Co., Ltd., Zhejiang, China. Emulsion polymerized styrene-butadiene rubber (ESBR, 1502, $M_n = 9.8 \times 10^4$, $M_w = 3.1 \times 10^5$) was offered by TSRC Co., Ltd., China. CB (N339) was supplied by Kabote (China) Investment Co., Ltd. Zinc oxide (ZnO) was purchased from US Zinc (Changshu) Co., Ltd., China. Stearic acid (SA) was obtained from Rugao Shuangma Chemical Co., Ltd., China. Aromatic hydrocarbon oil (VIVATEC 500) was provided by H & R China (Daxie) Co., Ltd. *N*-(1,3-Dimethylbutyl)-*N'*-phenyl-*p*-phenylenediamine (6-PPD), *N*-*tert*-butylbenzothiazole-2-sulphenamide (NS) and insoluble sulfur were obtained from Sunsine Chemical Co., Ltd., Shandong, China.

2.2 Preparation of the compounds

The two compounds investigated in this study were denoted as R and S, and their formulas are shown in Table 1. For the study of extrusion rheological behaviors of the compounds, the curing system was removed from the formula to ensure that the capillary would not be blocked by the cured rubber during the extrusion process at 100 °C. The compounds were prepared using an internal mixer (XSM-500, Shanghai Kechuang, China). The specifics are as follows. The rubbers and the ingredients were added in the first stage of internal mixing. The blends obtained were stored at room temperature for 4 h and then internally mixed again, and rubber compounds were obtained. The initial temperature and the mixing time for each sample are listed in Table 2. Furthermore, for the evaluation of the tensile properties of the composites, the compounds obtained were cured at 160 °C at a pressure of 10 MPa.

2.3 Measurements

The M_n and M_w of the rubbers were tested using a gel permeation chromatography (HLC 8320, Tosoh, Japan). The CB dispersity in the compounds was evaluated by a dispersion tester (disperGRADER α view, Alpha Technologies, USA). The bound rubber content (BRC) of the compounds was measured by toluene extraction as follows. The rubber compound was cut into small pieces, weighed (M_1 , approximately 0.5 g), and then placed into a wire nickel cage with a constant weight (M_2). Then, the sample was soaked in 100 mL toluene. After 48 h, the

Table 1 Formulas of R and S compounds

Component	Content/phr	
	S	R
NR	25	30
BR	50	70
ESBR	25	—
6-PPD	2	2
SA	2	2
ZnO	3	3
CB (N339)	30	70
Aromatic oil	10	5
NS ^a	1.5	2.5
Insoluble sulfur ^a	1.5	2.5

^a For the study of extrusion rheological behaviors of the compounds, the curing system, including the NS and the insoluble sulfur, was removed from the formula to ensure that the capillary would not be blocked by the cured rubber during the extrusion process at 100 °C.

toluene was replaced, and the sample was soaked for another 24 h. Then, the sample with the cage was removed, vacuum dried until its weight no longer changed, and weighed to obtain M_3 . The BRC was calculated according to eqn (1):

$$\text{BRC (\%)} = \frac{M_3 - M_2 - M_1 \times \alpha}{M_1 \times \beta} \times 100 \quad (1)$$

where α and β are the content percentages of the filler and the rubbers, respectively.

The viscoelasticity of the compounds was tested by strain sweep using a rubber process analyzer (RPA 2000, Alpha Technologies Co., USA). The strain amplitude range, frequency and temperature applied were 0.43%–100%, 1 Hz and 100 °C, respectively. The stress relaxation process of the compounds was also tracked by RPA under shear mode at various temperatures and shear strain for a time period of 120 s. Furthermore, tensile stress relaxation tests were conducted by a dynamic mechanical analyzer (DMA, TA instrument, Q800) at a fixed strain of 20% for 80 min at 25 °C and 100 °C.

The compounds obtained were extruded using a twin-bore capillary rheometer (Rosand RH 2000, Malvern Co., UK). One of the bores is equipped with a capillary, the length (L) and the diameter (D) of which are 16 mm and 1 mm, respectively. The other bore is fitted with a zero-length orifice die (L and D were 0.25 mm and 1 mm, respectively) for Bagley correction. The extrusion tests of the compounds were carried out at 100 °C at various shearing rates (γ_{as} , 5, 10, 20, 50, 100, 200, 500 and 1000 s^{-1}). The diameter of the extrudates (d) was measured by a stereoscopic microscope (Nikon SMZ 1500, Japan), and the die swell ratio (B) was calculated according to eqn (2):

$$B = \frac{d}{D} \quad (2)$$

where D is the diameter of the capillary (1 mm). The surface morphologies of the extrudates were also observed by stereoscopic microscopy. Three specimens were tested for the rheological behaviors for each sample.

Table 2 The initial mixing temperature and mixing time for each sample during the mixing process

	The first stage mixing process		The second stage mixing process	
	Initial temperature/°C	Mixing time/min	Initial temperature/°C	Mixing time/min
R-80	80	5.5	80	3.5
R-90	90	5.5	90	3.5
R-100	100	5.5	100	3.5
S-80	80	5.0	80	3.5
S-90	90	5.0	90	3.5
S-100	100	5.0	100	3.5

The tensile tests for the cured composites were conducted by a universal material testing machine (Z005, Zwick, Germany) at a drawing rate of 500 mm min⁻¹, and the tensile strength, elongation at break, and modulus at 100% and 300% elongation were obtained. Five specimens were tested for the evaluation of tensile properties.

3 Results and discussion

3.1 Mixing process

When the rubber and the ingredients were mixed in the internal mixer, heat was generated, and the temperature inside was elevated. With the temperature increase, the rubber is softened, and its flow capability is improved. However, an excessive

temperature, which normally occurs late in the process, is not conducive to mixing. In this case, further extension of the mixing time is not effective for the mixing uniformity but may aggravate the oxidative cleavage of the rubber molecule chains.^{41,42} To solve this problem, a multistage mixing process was invented and widely applied to ensure the mixing quality and performance requirements of the final products.⁴³ In this study, both samples R and S were prepared *via* a two-stage process.

Furthermore, heat generation during mixing was studied. As shown in Fig. 1, the heat generation of the R was much higher than that of the S, which should be due to the higher CB content in the sample R. As the initial temperature increased, the dumping temperature increased, and the heat generation of R

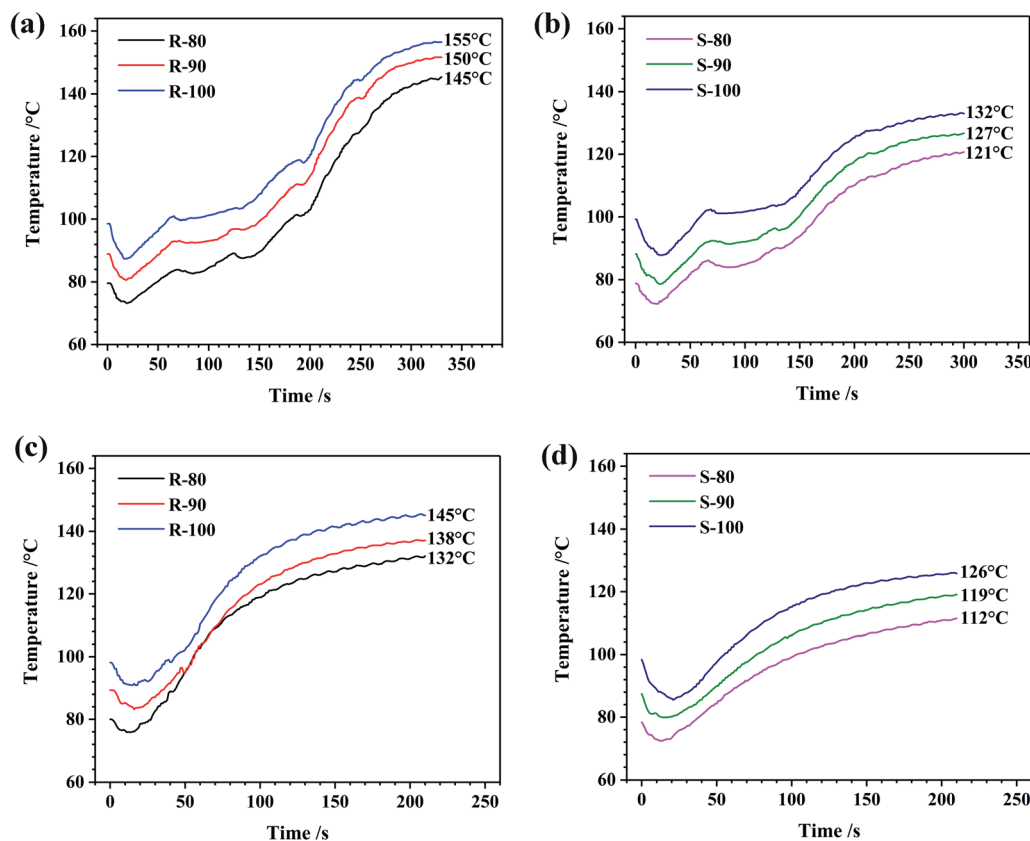


Fig. 1 Heat generation of the compounds prepared at various initial mixing temperatures as a function of mixing time ((a and b) the first stage mixing process for R and S, respectively; (c and d) the second stage mixing process for R and S, respectively).

was much higher than that of S when the initial temperature was the same. It is worth noting that the dumping temperature differences between R and S were basically the same regardless of the initial temperature. For example, when the initial mixing temperatures were 80–100 °C, the dumping temperature differences between R and S were 23–24 °C and 18–19 °C in the first and second stages, respectively. In general, it can be speculated that heat generation was mainly impacted by the formula of the compounds, whereas the initial temperature can be considered a minor factor influencing heat generation.

To evaluate the mixing uniformity of the compound, the CB dispersity in the matrix was observed. The images, which were transformed by numerical treatment into black-and-white mode, and the agglomerate sizes are shown in Fig. 2 and Table 3, respectively. As shown in Fig. 2, the CB agglomerates are highlighted as light dots, and the dark background is associated with the rubber matrix with well-dispersed CB. The CB aggregation in sample R was much more serious than that in sample S. This difference should be attributed to the high CB content of R. As the initial mixing temperature increased from 80 °C to 90 °C, the CB aggregation of R was mitigated, which indicated a higher mixing uniformity. However, when the mixing temperature was further raised to 100 °C, the mixing uniformity was not obviously changed. As mentioned above, when the mixing temperature was high, the flow capability of the compound increased, which was not conducive to the effects of the rotor on CB–CB interaction breaking. Furthermore, no remarkable difference was found for the mean agglomerate size of R at various mixing temperatures (Table 3).

To further discuss the interaction between the CB and the rubber molecular chain, the BRCs of the compounds were tested, and the results are listed in Table 4. The rubber bounded with the CB in the R was more than that in the S due to the higher CB content in the R. The initial mixing temperature in the range of 80–100 °C did not significantly affect the BRC of either R or S. Generally, the BRC slightly increased with the mixing temperature, indicating a minimally improved CB–rubber interaction.

Table 3 The agglomerate sizes of the compounds prepared at various initial mixing temperatures

	Agglomerate size/ μm
R-80	8.43 ± 4.40
R-90	8.25 ± 4.44
R-100	8.12 ± 4.29
S-80	10.12^a
S-90	8.62 ± 3.03
S-100	0^b

^a Only one observed light spot. ^b No observed light spots.

3.2 Stress relaxation

During the extrusion process, the polymer fluid was subjected to complex stress inside the capillary, for example, tensile and shear stress. The influences of the initial mixing temperature on the stress relaxation behavior of R and S under shear mode are shown in Fig. 3. Under shear mode, all the compounds, especially S, showed rapid stress relaxation. However, the initial mixing temperature did not significantly affect the pace of relaxation. The time for the torque to decrease to $1/e$ of the samples, as listed in Table 5, was within 0.4–0.5 s and 0.7–0.8 s for S and R, respectively.

Different from the results obtained under shear mode, the tensile stress relaxation rate was lower and more sensitive to the mixing temperature, which is shown in Fig. 4 and Table 6. As shown in Fig. 4(a), when tested at 25 °C, as the mixing temperature increased, the stress relaxation of both the R and S was obviously accelerated. This stress relaxation acceleration should be caused by the decrease in the rubber molecular weight and the improvement in CB dispersion. And the stress of the S dropped much more significantly. This should be due to the lower CB content in the S compound, which led to lower limitation on the rubber molecular chain. Furthermore, the tensile stress relaxation accelerated as the test temperature increased, and the relaxation rates of sample S became similar,

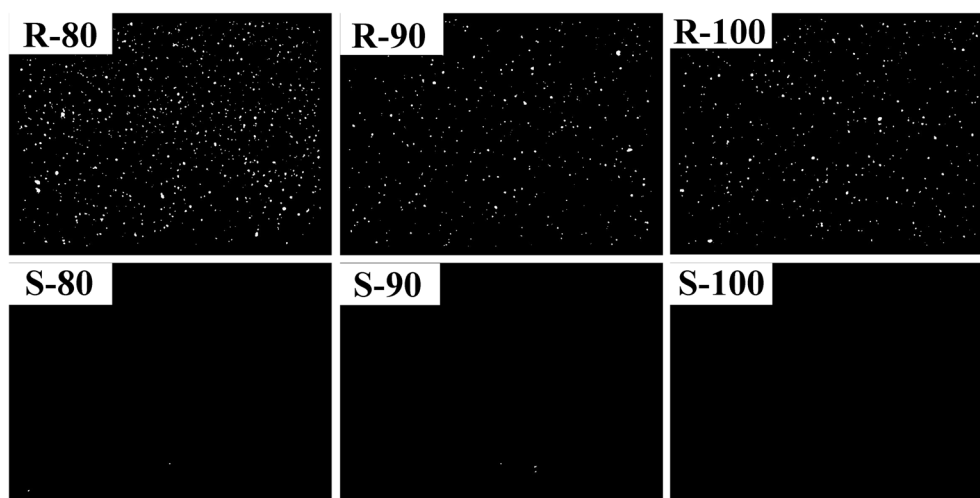


Fig. 2 CB dispersity images of the R and S compounds prepared at various initial mixing temperatures.

Table 4 BRCs of the compounds prepared at various initial mixing temperatures

	R-80	R-90	R-100	S-80	S-90	S-100
BRC/%	44.9 ± 0.36	45.6 ± 0.64	45.3 ± 0.54	26.4 ± 0.81	26.7 ± 0.87	27.3 ± 0.52

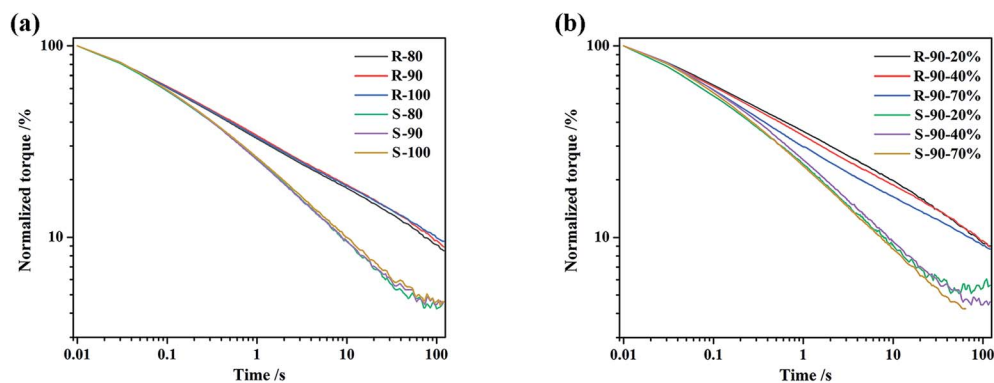


Fig. 3 The normalized torque curves of the compounds under shear mode ((a) strain 40%, temperature 60 °C; (b) temperature 60 °C).

Table 5 Stress relaxation time of the compounds under shear mode

Strain/%	Sample	$t_{1/e}^a/s$
40	R-80	0.7
	R-90	0.8
	R-100	0.7
	S-80	0.4
	S-90	0.4
	S-100	0.4
20	R-90	0.9
	S-90	0.3
70	R-90	0.5
	S-90	0.3

^a Time for the torque decreasing to $1/e$ of the initial torque.

whereas the rates of R mixed with various temperatures still showed large differences. It can be speculated that the stress relaxation rate change of S at 25 °C was mainly due to the slight

decrease in the rubber molecular weight as the mixing temperature rose. As the test temperature increased, the mobility of the molecular chain sharply increased, and thus, the stress relaxation rate became similar.

3.3 Dynamic strain sweep

To analyze the internal interactions of CB–CB under dynamic deformation, dynamic strain sweeps of samples R and S with various mixing temperatures were carried out by RPA. The dependence of the storage modulus (G') on the strain amplitude is shown in Fig. 5. Sample R showed a higher G' than that of S, especially at the initial stage with a low strain amplitude, which should be due to the stronger CB–CB interaction. As the strain amplitude increased, the G' of the R sharply decreased, which is described as the “Payne effect”, due to the breakup of the CB–CB network, and the CB–rubber interaction destruction and the disentanglement of the rubber molecular chains also contributed to this phenomenon. However, for S, a linear plateau

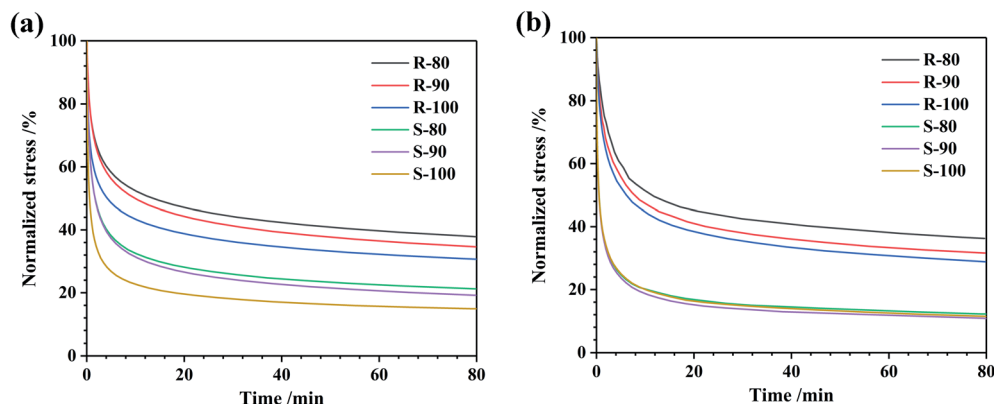
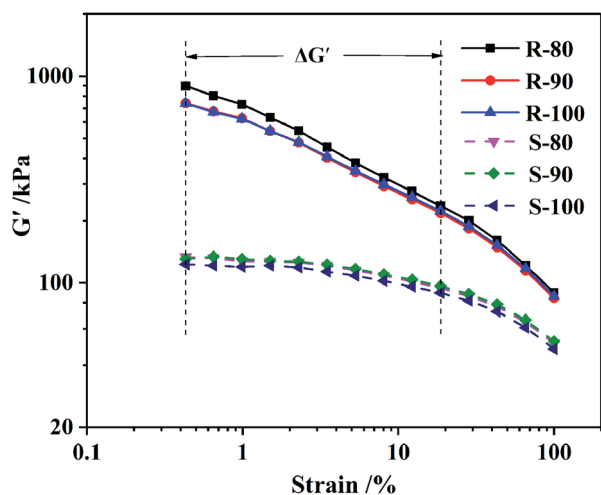


Fig. 4 Normalized stress relaxation curves of the compounds under tensile mode ((a) 25 °C; (b) 100 °C).

Table 6 Stress relaxation time of the compounds under tensile mode

Temperature/°C		$t_{1/e}/\text{min}$
25	R-80	>80.0
	R-90	55.0
	R-100	25.8
	S-80	5.8
	S-90	4.9
	S-100	1.6
100	R-80	75.1
	R-90	38.9
	R-100	27.0
	S-80	1.6
	S-90	1.3
	S-100	1.6

Fig. 5 Strain dependence of G' for the R and S compounds.

region at a low strain area can be observed, which was similar to the unfilled rubber materials. This phenomenon is due to the lower content and good dispersion of the CB inside the S samples (Fig. 2), which led to a lack of a CB–CB network. Therefore, the modulus variation at low strains ($\Delta G' = G'_{0.43\%} - G'_{18.65\%}$ in this study), as listed in Table 7, reflects the CB–CB network in the rubber matrix.

Furthermore, as the mixing temperature increased from 80 °C to 90 °C, G' in the low strain area decreased, but that at high strain remained relatively stable. Hence, the $\Delta G'$ decreased, which should be due to the improved CB dispersity. When the mixing temperature further increased to 100 °C, G' was not obviously affected. For sample S, the G' s and $\Delta G'$ s of the three samples were not significantly different since CB was highly uniformly dispersed regardless of the mixing temperature in the range of 80–100 °C. The slight decrease in the G' of S when the initial mixing temperature rises from 90 °C to 100 °C should be due to the rubber molecular weight decreasing.

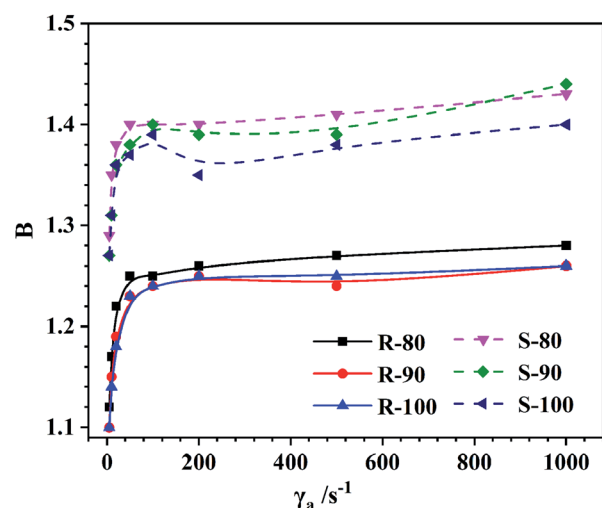
3.4 B and the appearance of the extrudates

Die swelling of the extrudate is a typical elastic behavior that occurs because of the recovery of elastic deformation imposed

Table 7 Effects of the initial mixing temperature on Payne effect ($\Delta G'$) of the R and S compounds

	$\Delta G' = G'_{0.43\%} - G'_{18.65\%}/\text{kPa}$
R-80	621 ± 57.4
R-90	534 ± 15.5
R-100	516 ± 0.3
S-80	35 ± 6.4
S-90	32 ± 3.5
S-100	32 ± 2.5

inside the capillary. The dependence of B on γ_a at 100 °C of the compounds is illustrated in Fig. 6. As γ_a increased, the B of both R and S initially sharply increased and then slowly increased. The increase in B with γ_a was the result of the increasing recoverable elastic energy stored in the melt flow. However, the dependence between B and γ_a decreased when γ_a was above 100 s^{-1} since the fluidity of the rubbers was relatively high at 100 °C. When the γ_a reached 1000 s^{-1} , the flow instability became much more severe, which led to significant distortion of the extrudates, especially for sample S (Fig. 7). In this case, the measured value of the extrudate diameter may have deviations to some extent. Generally, as the mixing temperature increased, although the CB dispersity and the BRCs remained basically unchanged, the B of the S obviously decreased. This phenomenon should be associated with the accelerated stress relaxation of the rubber molecular chains (Fig. 4) caused by the molecular weight reduction, which decreased the recovery of elastic deformation. However, for sample R, the increased CB content led to a relatively low elastic deformation ability, and the CB–rubber interaction degree became a major factor influencing B. With the mixing temperature increase, the stress relaxation of the rubber molecular chains significantly accelerated, but B initially decreased and then remained stable. This variation trend was similar to that of the CB dispersity and G' under low strain conditions.

Fig. 6 B of the compounds at various γ_a s (extrusion temperature: 100 °C).

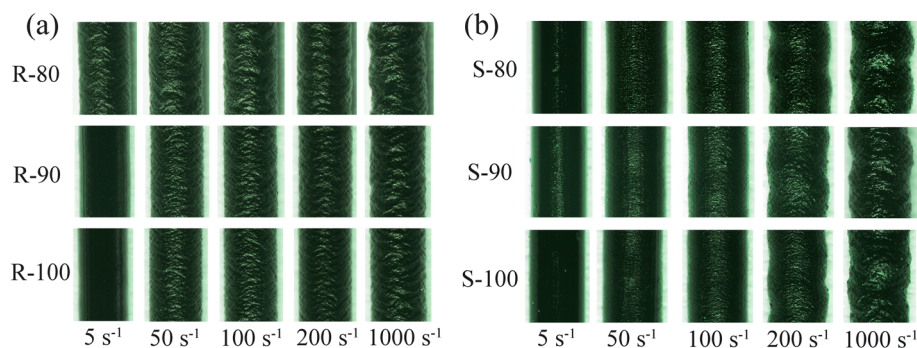


Fig. 7 Surface morphologies of the extrudates at various $\gamma_a s$ ((a) R; (b) S).

Table 8 Tensile properties of the cured R and S composites

Samples	Tensile strength/MPa	Elongation at break/%	100% modulus/MPa	300% modulus/MPa
R-80	18.3 ± 1.28	223 ± 16.5	5.7 ± 0.08	— ^a
R-90	18.8 ± 0.33	221 ± 11.9	6.0 ± 0.33	— ^a
R-100	18.1 ± 0.88	213 ± 12.7	6.0 ± 0.17	— ^a
S-80	15.1 ± 0.39	561 ± 10.2	1.1 ± 0.02	4.6 ± 0.15
S-90	14.9 ± 0.76	562 ± 22.6	1.1 ± 0.02	4.6 ± 0.17
S-100	15.1 ± 0.55	593 ± 5.1	1.1 ± 0.03	4.2 ± 0.03

^a The elongation at break of the R was less than 300%.

Furthermore, the appearances of the extrudates are compared in Fig. 7. For R-80, all the extrudates with various extruding rates show obvious sharkskin due to the surface instability. Slight global distortion can also be observed when the apparent γ_a reaches 1000 s^{-1} . As the mixing temperature increased, the sharkskin appearance was mitigated, which should be due to the improved CB dispersity. For sample S, the flow instability was more severe than that of sample R due to the lower content of CB and the presence of ESBR with a large side group; thus, integral distortion occurred when the γ_a was above 200 s^{-1} . As the mixing temperature increased, the appearance state of the S was also improved.

3.5 Tensile properties of the vulcanizates

The tensile properties of the vulcanizates are very important for the rubber materials in actual applications.^{44–46} The tensile properties of the cured R and S are listed in Table 8. Compared with the S, sample R was with higher tensile strength and modulus but lower elongation at break due to its high CB content. However, the mixing temperature change in the range of 80 °C to 100 °C has little effect on the tensile properties of the vulcanizates. In other words, the tensile properties of the vulcanizates were less sensitive to the mixing temperature than the extrusion rheological behaviors of both the uncured R and S compounds.

4 Conclusions

In this paper, a two-stage mixing process was used to prepare rim strip (R) and sidewall (S) compounds with initial mixing

temperatures of 80, 90 and 100 °C. The effects and mechanism of the mixing temperature on the rheological behaviors of the two compounds were different due to their different structures. R had a high carbon black (CB) content, and the CB dispersity was the main factor, whereas for S with a low CB content, the rubber molecular weight decrease during mixing became the determining factor. The stress relaxation rates under tensile mode of both R and S were more sensitive to the mixing temperature than the rates under shear mode. Strain sweep results obtained by RPA showed that R had a more obvious Payne effect than S. When the initial mixing temperature increased from 80 °C to 90 °C, both G' and $\Delta G'$ at low shear strain decreased, indicating CB dispersion improvement. Furthermore, the B of the S extrudates was higher and more sensitive to the mixing temperature than that of the R extrudates. As the mixing temperature increased, the B of S obviously decreased, whereas the B of R initially decreased and then remained basically unchanged. In addition, the increased mixing temperature was conducive to the improvement of the extrudate surfaces.

Conflicts of interest

There are no conflicts to declare.

References

- 1 C. Abeykoon, *Control Eng. Pract.*, 2016, **51**, 69.
- 2 C. Sirisinha, *J. Sci. Soc. Thailand*, 1997, **23**, 259.

- 3 P. G. Lafleur and B. Vergnes, *Polymer extrusion*, John Wiley & Sons, Hoboken, 2014.
- 4 T. Z. Zaeimoedin, M. Mustafa Kamal and A. K. Che Aziz, *Adv. Mater. Res.*, 2016, **1133**, 236.
- 5 M. R. Kashani, *J. Appl. Polym. Sci.*, 2009, **113**, 1355.
- 6 C. McAfee, J. A. Whidden and M. L. Dulisse, *US Pat.*, 9868844B2, 2018.
- 7 Y. K. Dai, H. Zheng, C. X. Zhou and W. Yu, *J. Macromol. Sci., Part A: Pure Appl. Chem.*, 2008, **45**, 1028.
- 8 Y. S. Ha, J. R. Cho, T. H. Kim and J. H. Kim, *J. Mater. Process. Technol.*, 2008, **201**, 168.
- 9 A. Goldshtein, G. Vavilova, A. Rumkin and O. Starý, *Mater. Sci. Forum*, 2019, **942**, 141.
- 10 L. A. Goettler, A. J. Lambright, R. I. Leib and P. J. Dimauro, *Rubber Chem. Technol.*, 1981, **54**, 277.
- 11 R. J. Pazur and T. A. C. Kennedy, *Rubber Chem. Technol.*, 2015, **88**, 324.
- 12 A. Bandyopadhyay, M. De Sarkar and A. K. Bhowmick, *Rubber Chem. Technol.*, 2005, **78**, 806.
- 13 G. He, T. Luo, Y. G. Dang, L. Zhou, Y. Y. Dai and X. Ji, *RSC Adv.*, 2021, **11**, 817.
- 14 C. Yang and Z. R. Li, *J. Appl. Polym. Sci.*, 2016, **133**, 43522.
- 15 A. M. Yousefi and H. Atspha, *Polym. Eng. Sci.*, 2009, **49**, 229.
- 16 N. C. Das, H. Wang, J. Mewis and P. Moldenaers, *J. Polym. Sci., Part B: Polym. Phys.*, 2005, **43**, 3519.
- 17 S. Ganguly and N. C. Das, in *Carbon-Containing Polymer Composites*, ed. M. Rahaman *et al.*, Springer, Singapore, 2019, p. 271.
- 18 G. M. C. Alwis, N. Kottegoda and U. N. Ratnayake, *Appl. Clay Sci.*, 2020, **191**, 105633.
- 19 S. Sadhu and A. K. Bhowmick, *J. Polym. Sci., Part B: Polym. Phys.*, 2005, **43**, 1854.
- 20 Z. Y. Zhu, *Rheol. Acta*, 2004, **43**, 373.
- 21 A. K. Zachariah, V. G. Geethamma, A. K. Chandra, P. K. Mohammed and S. Thomas, *RSC Adv.*, 2014, **4**, 58047.
- 22 N. Rattanasom and K. Suchiva, *J. Appl. Polym. Sci.*, 2005, **98**, 456.
- 23 S. Patcharaphun, Y. Sukniyom, W. Chookaew and N. Sombatsompop, *Prog. Rubber, Plast. Recycl. Technol.*, 2014, **30**, 129.
- 24 M. Nanda and D. K. Tripathy, *J. Appl. Polym. Sci.*, 2012, **126**, 46.
- 25 A. Crié, C. Baritaud, R. Valette and B. Vergnes, *Polym. Eng. Sci.*, 2015, **55**, 2156.
- 26 R. Niu, J. Gong, D. H. Xu, T. Tang and Z. Y. Sun, *RSC Adv.*, 2014, **4**, 62759.
- 27 Z. Wang, Y. Han, Z. H. Huang, X. Zhang, L. Q. Zhang, Y. L. Lu and T. W. Tan, *J. Appl. Polym. Sci.*, 2014, **131**, 40643.
- 28 Y. Q. Ren, S. H. Zhao, Q. Q. Li, X. Y. Zhang and L. Q. Zhang, *J. Appl. Polym. Sci.*, 2015, **132**, 41485.
- 29 J. Li, Master Degree thesis, Qingdao University of Science and Technology, 2018.
- 30 K. Kubota, R. Brzoskowski, J. L. White, F. C. Weissert, N. Nakajima and K. Min, *Rubber Chem. Technol.*, 1987, **60**, 924.
- 31 J. W. G. Main, PhD thesis, Martin Luther University Halle-Wittenberg, 2010.
- 32 S. Brockhaus and V. Schöppner, *Int. Polym. Sci. Technol.*, 2015, **42**, 1.
- 33 P. Elmiawan, H. Saryanto and D. Sebayang, *IOP Conf. Ser.: Mater. Sci. Eng.*, 2017, **204**, 012020.
- 34 M. Meysami, C. Tzoganakis, P. Mutyala, S. H. Zhu and M. Bulsari, *Int. Polym. Process.*, 2017, **32**, 183.
- 35 S. Sharma, K. Sarkar, M. Goswami, A. Deb, S. Dcunha and S. Chattopadhyay, *J. Manuf. Process.*, 2020, **57**, 700.
- 36 M. J. Vilorio, M. Valtier and B. Vergnes, *J. Rheol.*, 2017, **61**, 1085.
- 37 R. Plachy, S. Scheiner, K. W. Luczynski, A. Holzner and C. Hellmich, *Polymer*, 2017, **123**, 334.
- 38 S. Stieger, R. C. Kerschbaumer, E. Mitsoulis, M. Fasching, G. R. Berger-Weber, W. Friesenbichler and J. Sunder, *Polym. Eng. Sci.*, 2020, **60**, 32.
- 39 K. Sankaran, G. B. Nando, P. Ramachandran, S. Nair, U. Govindan, S. Arayambath and S. Chattopadhyay, *RSC Adv.*, 2015, **5**, 87864.
- 40 U. Quintavalle, D. Voinovich, B. Perissutti, F. Serdoz, G. Grassi, A. Dal Col and M. Grassi, *Eur. J. Pharm. Sci.*, 2008, **33**, 282.
- 41 M. Pike and W. F. Watson, *J. Polym. Sci.*, 1952, **9**, 229.
- 42 R. F. Ohm, in *Mixing of Rubber*, ed. R. H. Grossman, Chapman & Hall, London, 1997, ch. 6, p. 91.
- 43 Q. Z. Yang, *Practical Rubber Technology*, Chemical Industry Press, Beijing, 2005.
- 44 S. Ganguly, P. Bhawal, A. Choudhury, S. Mondal, P. Das and N. C. Das, *Polym.-Plast. Technol. Eng.*, 2018, **57**, 997.
- 45 Z. Yang, Y. Huang and Y. Z. Xiong, *RSC Adv.*, 2020, **10**, 41857.
- 46 L. P. Qin, Y. M. Zhang, Y. F. Zhang and Y. B. Gong, *Appl. Clay Sci.*, 2021, **213**, 106237.